ChemComm

COMMUNICATION

View Article Online
View Journal | View Issue

Cite this: *Chem. Commun.*, 2023, 59, 14803

Received 20th September 2023,
Accepted 20th November 2023

DOI: 10.1039/d3cc04656g

rsc.li/chemcomm

Accurate assessment of electrocatalytic carbon dioxide reduction products at industrial-level current density†

Xin Zi, ‡[a] Qiuwen Liu,‡[a] Li Zhu,[b] Qin Chen,[a] Xiangqiong Liao,[a] Ziwen Mei,[a] Xiaojian Wang,[a] Xiqing Wang,[a] Kang Liu,[a] Junwei Fu *[a] and Min Liu *[a]

During the electrocatalytic CO_2 reduction reaction, the faradaic efficiency of products seriously deviates from 100% due to the misjudgment of outlet flow, especially at industrial-level large current density. In this work, several modified equations and internal standard methods are recommended to calibrate the thermal mass flowmeter and establish benchmarks for CO_2 reduction performance assessment.

The electrocatalytic CO_2 reduction reaction (CO_2RR) is a potential strategy to achieve carbon neutrality.[1–6] The industrial applications of CO_2RR require target products with high selectivity and large current density.[7–11] Over the past few decades, great efforts have been devoted to developing efficient catalysts and devices, especially for improving the current density and faradaic efficiency (FE) of multi-carbon (C_{2+}) products.[12–17] As a result, industrial-level large current density (>500 mA cm^{-1}) for the CO_2RR in flow cell systems has been widely reported.[18–23] However, several parameters in evaluating the FE at such high current density are commonly overlooked, resulting in the total FE deviating from 100%, and thus unreliable assessment of CO_2RR performance.[6,24–27]

During the CO_2RR under industrial-level current density in a flow cell, the conversion of CO_2 to the product and hydrogen evolution reaction lead to obvious changes of the gas flow rate at the outlet.[28–30] Real-time monitoring of the outlet flow rate is necessary for accurate FE calculation.[31–33] Thermal mass flowmeters, which are not affected by gas pressure and temperature, have been widely used to measure gas mass flow rate with high accuracy.[34] Unluckily, gas components with different thermodynamic properties generally lead to large deviations between the actual flow rate and the indicated flow rate. In order to accurately measure the flow rate, the thermal mass flowmeter must be calibrated according to the components of the gas. Therefore, developing a simple method to accurately measure the gas flow rate at the outlet is the basis for reliable FE calculation of the gas products.

In this work, we propose a series of methods to calibrate the FE, including (1) using a suitable range of flowmeter to measure the gas flow rate; (2) deducing the revised equations to calibrate the gas flow rate; (3) applying a gas internal standard method to measure the outlet flow rate. Our experimental results show that the above methods can correct the misestimation of the products to 100% FE.

Fig. 1 exhibits the schematic diagram of the CO_2 electroreduction process in a flow cell device, which mainly consists of a gas chamber, a cathode chamber, and an anode chamber.[35,36] The products will migrate between different chambers at high current density. Gas products will accumulate at the surface of the catalyst layer at high current density, and be washed away

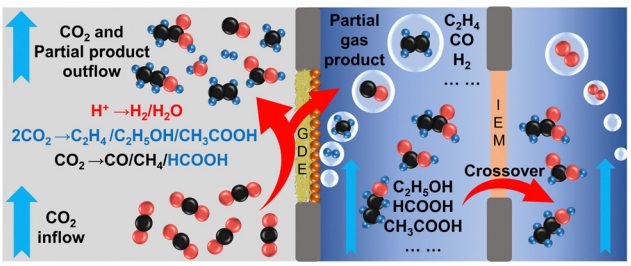

Fig. 1 Schematic diagram of the CO_2 electroreduction process in a flow cell device. From left to right are gas chamber, cathode chamber, and anode chamber, respectively. The black, red, and blue spheres represent carbon, oxygen, and hydrogen atoms, respectively. The brown spheres in the GDE represent the catalyst layer, and the blue arrows represent the flow direction.

[a] *Hunan Joint International Research Center for Carbon Dioxide Resource Utilization, School of Physics and Electronics, Central South University, Changsha 410083, Hunan, P. R. China. E-mail: fujunwei@csu.edu.cn, minliu@csu.edu.cn*

[b] *Nanoinstitut München, Fakultät für Physik, Ludwig-Maximilians-Universität München, München 80539, Germany*

† Electronic supplementary information (ESI) available. See DOI: https://doi.org/10.1039/d3cc04656g

‡ These authors contributed equally.

by the flowing cathode electrolyte. Most important of all, the products and the absorption of CO_2 by the electrolyte can cause changes of the outlet flow rate (Fig. S1, ESI†), which is an important parameter for calculating the FE of gas products.

Eqn (1) is used to calculate the FE of gas products detailed derivation of the process in the ESI,† eqn (S1)–(S5).

$$FE_i = \frac{N_i P \nu C_i F}{IRT} \quad (1)$$

According to eqn (1), the outlet flow ν directly affects the calculation of FE. Accurate measurement of gas outlet flow is the basis of FE calculation and CO_2RR performance evaluation. At present, the thermal mass flowmeter is the most used device for real-time monitoring of outlet flow.

As shown in Fig. 2a, the thermal mass flowmeter measures the flow rate of gas by capillary heat transfer and temperature difference calorimetry. Specifically, the flow rate value is obtained by heating the flowing gas, transferring the heat downstream, and then measuring the temperature difference between the upstream and downstream. Although the thermal mass flowmeter will not be affected by temperature and pressure, the measurement of mixed gases with different thermodynamic properties will cause large errors.

In order to reduce the error, many aspects must be considered. Firstly, the accuracy is often closely related to the full range of the flowmeter. A large error occurs when using a large-range flowmeter to measure a small flow rate. As shown in Fig. 2b, when the actual flow rate is less than 10 sccm, the use of a flowmeter with the range of 50 or 100 sccm (standard cubic centimeter per minute) produces an error far greater than that of a flowmeter with a range of 10 sccm (Fig. S2, ESI†). Secondly, for gas mixtures, it is not easy to calibrate flowmeters with a certain conversion coefficient (Fig. 2c). According to the principle of the thermal mass flowmeter, the flow rate of mixed gases with different components can be converted by different conversion coefficients separately, and then the total flow rate can be summarized. In this case, the proportion of different gases must be known. However, the proportion of the gas mixture changes in real-time during the CO_2RR, and it is impossible to calibrate the flow rate with a fixed coefficient. Fortunately, the proportion of the gas mixture can be measured by gas chromatography (GC) in real-time. On this basis, we derived eqn (2) to correct the error of the indicated flow rate in the thermal mass flowmeter.

$$\nu_{actual} = \frac{\nu_{indicated}}{\sum_i \frac{C_i}{10^6}\frac{B_{CO_2}}{B_i} + \frac{10^6 - \sum_i C_i}{10^6}} \quad (2)$$

where ν_{actual} is the calculated actual flow rate (sccm), $\nu_{indicated}$ is the flow rate displayed by the thermal mass flowmeter (sccm), C_i is the concentration of component i (except CO_2) measured by GC (ppm), and B_{CO_2} and B_i are the conversion coefficients of CO_2 and component i. (Detailed derivation of the process can be found in the ESI,† eqn (S6)–(S10)).

To verify the applicability of eqn (2), we compared the calculation error by eqn (2) and the actual experimental error. As shown in Fig. S3 (ESI†), the known flow rates of CO_2 and H_2 are mixed into the thermal mass flowmeter (calibrated by CO_2) to obtain the displayed flow rate, while the actual flow rate is measured by the soap film flowmeter. The flow errors of the mixture gases of H_2 and CO_2 with different ratios are shown in Fig. 2d (red dots).

The theoretical errors calculated by the above equation are shown as the black dotted line. These results show that eqn (2) can correct the measurement error caused by the real-time change of the gas mixture measured by the thermal mass flowmeter.

Furthermore, we used eqn (2) to predict the flow rate error of the thermal mass flowmeter. The different proportions of gas products were mixed with the CO_2 gas, and the thermal mass flowmeter was calibrated with CO_2 gas (Fig. 3a). The results show that as the concentration of H_2 or CO increases, the flow rate of the gas mixture will significantly be underestimated by up to 26.7%. In contrast, if the gas product C_2H_4 increases, the flow rate will be overestimated by up to 21.3%. The conversion coefficient of CH_4 (0.785) is closer to that of CO_2 (0.74), while the flow rate will be underestimated by up to 5.7% as the proportion of CH_4 increases.

At a low CO_2 supply flow rate, the impact of flowmeter errors will be further amplified. At present, in order to pursue high single-pass carbon efficiency in acidic electrolytes, the CO_2RR is often measured at a low flow rate (below 10 sccm). The lower the CO_2 flow rate, the higher the concentration of the products, and then the greater the error. In Fig. 3b, the catalyst with CO_2RR performance of FE_{CO} = 95%, FE_{H_2} = 5% is taken as an example. With increasing current, the relative concentration of CO and H_2 in the mixture of CO_2 gas increases, and then the

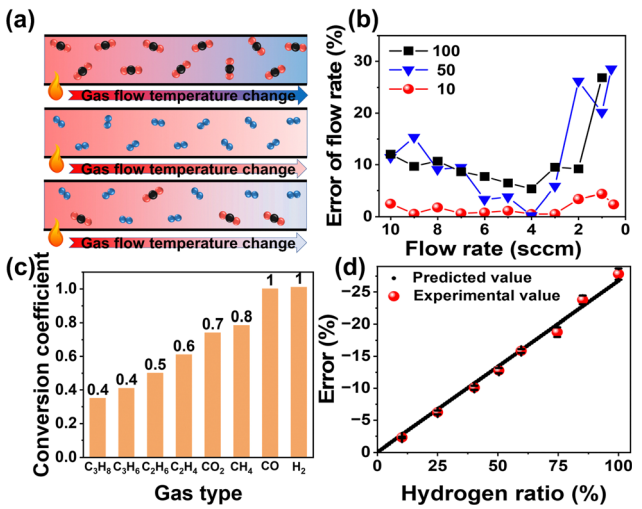

Fig. 2 (a) Schematic diagram of the temperature profile of CO_2, H_2, and CO_2/H_2 mixture gas at the same flow rate in thermal mass flowmeters. The arrows represent the direction of gas flow. (b) Measurement errors of thermal mass flowmeters with different ranges for low flow rate of gas. (c) Conversion coefficients of thermal mass flowmeters for different gases. (d) The flow errors of the mixture gases of H_2 and CO_2 with different ratios, measured by a CO_2 calibrated thermal mass flowmeter.

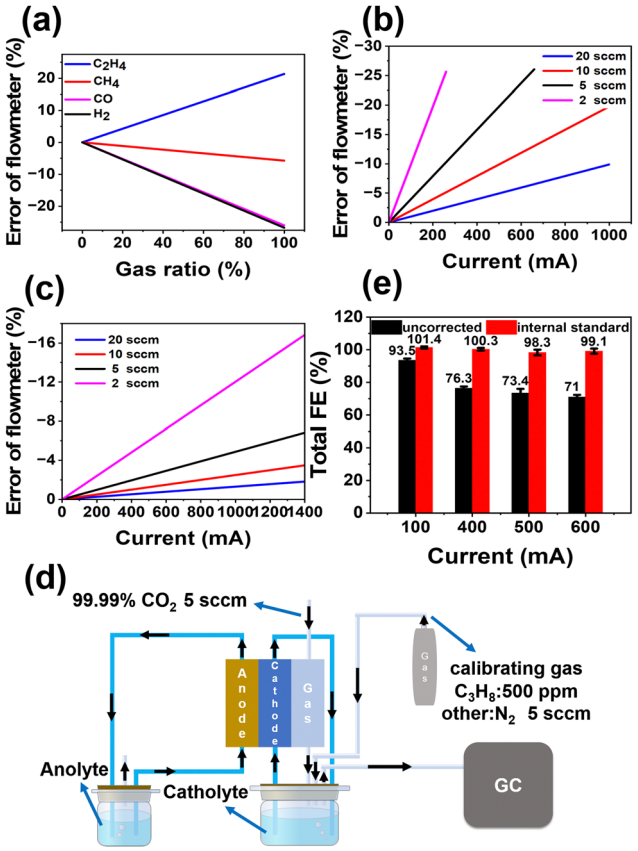

Fig. 3 (a) The error of the flowmeter with different proportions of single gas product mixed with CO_2 gas. (b) The error of the flowmeter with different CO_2 supply flow and different current in FE_{CO} = 95%, FE_{H_2} = 5% product mixture gases. (c) The error of the flowmeter with the different CO_2 supply flow and different current in $FE_{C_2H_4}$ = 60%, FE_{CH_4} = 20%, FE_{CO} = 10%, FE_{H_2} = 10% product mixture gases. All the thermal mass flowmeters were calibrated with CO_2 gas. (d) The schematic diagram of the device for calculating outlet flow by the internal (C_3H_8) standard method. (e) The FE calculated by the inlet flow rate (black) and outlet flow rate measured by the internal standard method (red).

error of the flowmeter (calibrated by CO_2) increases. When the flow rate is reduced to 2 sccm and the current is increased to 200 mA, the CO_2 conversion rate is close to 100%. The mixed gases at the outlet are 95% CO and 5% H_2 (no CO_2 gas), and the flow rate will be underestimated by 26%. Under the same current, the higher CO_2 supply flow rate makes the product (CO and H_2) concentration lower, which indicates that most of the gas at the outlet is CO_2, and the error of the flowmeter will be greatly reduced. When the flow rate reaches 20 sccm, even if the current reaches 1000 mA, the error of the flow rate at the outlet is less than 10%.

Furthermore, we considered the case of more complex products in the CO_2RR. The catalyst with CO_2RR performance of $FE_{C_2H_4}$ = 60%, FE_{CH_4} = 20%, FE_{CO} = 10%, FE_{H_2} = 10% is taken as an example. Since the error effect of C_2H_4 is opposite to CH_4, H_2 and CO on the CO_2 calibrated flowmeter, they will compensate each other, and the total error of the thermal mass flowmeter will be alleviated. As shown in Fig. 3c, when the flow rate is reduced to 2 sccm and the current rises to 1400 mA, the error of the flow rate at the outlet is more than 16%. In brief, it is important to acknowledge the outlet flow error at high current and low CO_2 supply flow rate, and we should utilize a revised formula to calibrate the mass flowmeter's results.

In addition, the instrumental measurement limitations of GC must be considered when detecting the gas products with high concentrations. Most GCs are designed to measure products at specific concentrations, while there are large deviations for other concentration ranges. For unknown gas products with high concentrations, a standard curve calibration at new high concentrations is required. Moreover, when the flow rate is too low, the large dead volume between the flow cell and the GC presents an obstacle to accurately measure the product concentration. Fortunately, the internal standard method can solve these problems perfectly. By adding a standard carrier gas with known non-product substance to the gas product outlet, not only can the low flow rate of gas products be smoothly transported into the GC for measurement (Fig. 3d), but also the actual flow rate can be calculated by the GC-detected concentration value of the non-product substance. The principle is that the stable standard carrier gas is diluted by the gas product, the concentration of the standard carrier gas changes with the product flow rate (detailed derivation of the process shown in the ESI† eqn (S11)–(S13)):

$$\nu_{\text{actual}} = \frac{c_{x0}}{c_x}\nu_x \tag{3}$$

where: ν_{actual} is the calculated flow rate of the mixture of product and carrier gas (sccm); ν_x is the flow rate of the standard carrier gas (sccm); c_{x0} is the known concentration of the standard carrier gas (ppm); c_x is the measured value of the concentration of the standard carrier gas by GC (ppm).

In addition, the internal standard method can also effectively eliminate GC concentration error caused by gas pressure change (the details are shown in the ESI†). Using a typical catalyst whose CO_2RR products are CO and H_2, the internal standard experiment (Fig. 3e) shows that the FE will be closer to 100%. While the FE gradually deviates from 100% with a gradual increase of the current by directly using the inlet flow rate for calculation.

In this work, we focus on the issue that the FE of CO_2RR products seriously deviates from 100% at high current density. The outlet flow rate of the gas product and the dead volume of the liquid pipeline are critical. Firstly, the principle of thermal mass flowmeter is analyzed, the test error of mixed gases is summarized, and the gas flow rate is corrected by the modified equations. Furthermore, the internal standard method is introduced to accurately calibrate the flow rate, and solve the measurement problem of low flow rate and high-concentration products. This is particularly important for the measurement of single-pass carbon efficiency. In general, the FE of all products can be accurately measured by the above modified methods, which provides a reliable scheme for accurate evaluation of products under industrial-level current density.

Xin Zi: conceptualization, writing – original draft, Qiuwen Liu: conceptualization, Li Zhu: resource, Qin Chen: investigation, Xiangqiong Liao: visualization, Ziwen Mei: data curation, Xiaojian Wang: validation, Xiqing Wang: data curation, Kang Liu: supervision, Junwei Fu: conceptualization, project administration, writing – review & editing, Min Liu: supervision, funding acquisition, writing – review & editing.

The authors gratefully acknowledge the National Natural Science Foundation of China (Grant No. 22376222, 52372253, 22002189), the Science and Technology Innovation Program of Hunan Province (2023RC1012), Central South University Research Programme of Advanced Interdisciplinary Studies (Grant No. 2023QYJC012), and Central South University Innovation-Driven Research Programme (Grant No. 2023CXQD042). We are grateful for resources from the High Performance Computing Center of Central South University.

Conflicts of interest

There are no conflicts to declare.

Notes and references

1 C. Guo, S. Liu, Z. Chen, B. Li, L. Chen, C. V. Singh, B. Liu and Q. Mao, *Chem. Commun.*, 2021, **57**, 1384–1387.
2 K. Jiang, Y. Huang, G. Zeng, F. M. Toma, W. A. Goddard III and A. T. Bell, *ACS Energy Lett.*, 2020, **5**, 1206–1214.
3 Y. Zhou, Y. Liang, J. Fu, K. Liu, Q. Chen, X. Wang, H. Li, L. Zhu, J. Hu, H. Pan, M. Miyauchi, L. Jiang, E. Cortes and M. Liu, *Nano Lett.*, 2022, **22**, 1963–1970.
4 L. Zhu, Y. Lin, K. Liu, E. Cortés, H. Li, J. Hu, A. Yamaguchi, X. Liu, M. Miyauchi, J. Fu and M. Liu, *Chin. J. Catal.*, 2021, **42**, 1500–1508.
5 K. Chen, M. Cao, G. Ni, S. Chen, H. Liao, L. Zhu, H. Li, J. Fu, J. Hu, E. Cortés and M. Liu, *Appl. Catal., B*, 2022, **306**, 121093.
6 Y. Rong, J. Sang, L. Che, D. Gao and G. Wang, *Acta Phys.-Chim. Sin.*, 2023, **39**, 2212027.
7 Q. Chen, K. Liu, Y. Zhou, X. Wang, K. Wu, H. Li, E. Pensa, J. Fu, M. Miyauchi, E. Cortes and M. Liu, *Nano Lett.*, 2022, **22**, 6276–6284.
8 K. Liu, J. Fu, L. Zhu, X. Zhang, H. Li, H. Liu, J. Hu and M. Liu, *Nanoscale*, 2020, **12**, 4903–4908.
9 X. Zi, Y. Zhou, L. Zhu, Q. Chen, Y. Tan, X. Wang, M. Sayed, E. Pensa, R. A. Geioushy, K. Liu, J. Fu, E. Cortes and M. Liu, *Angew. Chem., Int. Ed.*, 2023, e202309351.
10 Q. Chen, X. Wang, Y. Zhou, Y. Tan, H. Li, J. Fu and M. Liu, *Adv. Mater.*, 2023, e2303902.
11 N. Wang, R. K. Miao, G. Lee, A. Vomiero, D. Sinton, A. H. Ip, H. Liang and E. H. Sargent, *SmartMat*, 2021, **2**, 12–16.
12 H. Xiong, J. Li, D. Wu, B. Xu and Q. Lu, *Chem. Commun.*, 2023, **59**, 5615–5618.
13 Z. Yin, C. Yu, Z. Zhao, X. Guo, M. Shen, N. Li, M. Muzzio, J. Li, H. Liu, H. Lin, J. Yin, G. Lu, D. Su and S. Sun, *Nano Lett.*, 2019, **19**, 8658–8663.
14 M. Zheng, P. Wang, X. Zhi, K. Yang, Y. Jiao, J. Duan, Y. Zheng and S. Z. Qiao, *J. Am. Chem. Soc.*, 2022, **144**, 14936–14944.
15 K. Yang, Y. Sun, S. Chen, M. Li, M. Zheng, L. Ma, W. Fan, Y. Zheng, Q. Li and J. Duan, *Small*, 2023, **19**, e2301536.
16 X. Wang, Q. Chen, Y. Zhou, Y. Tan, Y. Wang, H. Li, Y. Chen, M. Sayed, R. A. Geioushy, N. K. Allam, J. Fu, Y. Sun and M. Liu, *Nano Res.*, 2023, DOI: 10.1007/s12274-023-5910-9.
17 H. Xu, X. Song, Q. Zhang, C. Yu and J. Qiu, *Acta Phys.-Chim. Sin.*, 2024, **40**, 2303040.
18 Y. Xie, P. Ou, X. Wang, Z. Xu, Y. C. Li, Z. Wang, J. E. Huang, J. Wicks, C. McCallum, N. Wang, Y. Wang, T. Chen, B. T. W. Lo, D. Sinton, J. C. Yu, Y. Wang and E. H. Sargent, *Nat. Catal.*, 2022, **5**, 564–570.
19 Z. Ma, Z. Yang, W. Lai, Q. Wang, Y. Qiao, H. Tao, C. Lian, M. Liu, C. Ma, A. Pan and H. Huang, *Nat. Commun.*, 2022, **13**, 7596.
20 J. Gu, S. Liu, W. Ni, W. Ren, S. Haussener and X. Hu, *Nat. Catal.*, 2022, **5**, 268–276.
21 J. E. Huang, F. Li, A. Ozden, A. Rasouli and F. P. G. D. Arquer, *Science*, 2021, **13**, 7596.
22 Y. Zhao, L. Hao, A. Ozden, S. Liu, R. K. Miao, P. Ou, T. Alkayyali, S. Zhang, J. Ning, Y. Liang, Y. Xu, M. Fan, Y. Chen, J. E. Huang, K. Xie, J. Zhang, C. P. O'Brien, F. Li, E. H. Sargent and D. Sinton, *Nat. Synth.*, 2023, **2**, 403–412.
23 T. Tang, Z. Wang and J. Guan, *Acta Phys.-Chim. Sin.*, 2022, **39**, 2208033.
24 Q. Wang, K. Liu, J. Fu, C. Cai, H. Li, Y. Long, S. Chen, B. Liu, H. Li, W. Li, X. Qiu, N. Zhang, J. Hu, H. Pan and M. Liu, *Angew. Chem., Int. Ed.*, 2021, **60**, 25241–25245.
25 J. E. Huang, F. Li, A. Ozden, A. Sedighian Rasouli, F. P. Garcia de Arquer, S. Liu, S. Zhang, M. Luo, X. Wang, Y. Lum, Y. Xu, K. Bertens, R. K. Miao, C. T. Dinh, D. Sinton and E. H. Sargent, *Science*, 2021, **372**, 1074–1078.
26 D. Xu, Y. Xu, H. Wang and X. Qiu, *Chem. Commun.*, 2022, **58**, 3007–3010.
27 S. Chen, X. Li, C. W. Kao, T. Luo, K. Chen, J. Fu, C. Ma, H. Li, M. Li, T. S. Chan and M. Liu, *Angew. Chem., Int. Ed.*, 2022, **61**, e202206233.
28 Z. Niu, L. Chi, R. Liu, Z. Chen and M. Gao, *Energy Environ. Sci.*, 2021, **14**, 4169–4176.
29 G. O. Larrazábal, M. Ming and S. Brian, *Acc. Mater. Res.*, 2021, **2**, 220–229.
30 Q. Wang, K. Liu, K. Hu, C. Cai, H. Li, H. Li, M. Herran, Y. R. Lu, T. S. Chan, C. Ma, J. Fu, S. Zhang, Y. Liang, E. Cortes and M. Liu, *Nat. Commun.*, 2022, **13**, 6082.
31 J. Zhang, W. Luo and A. Züttel, *J. Catal.*, 2020, 140–145.
32 P. A. Kempler and A. C. Nielander, *Nat. Commun.*, 2023, **14**, 1158.
33 C. J. Bondue, M. Graf, A. Goyal and M. T. M. Koper, *J. Am. Chem. Soc.*, 2021, **143**, 279–285.
34 G. Chen, H. Li, Y. Zhou, C. Cai, K. Liu, J. Hu, H. Li, J. Fu and M. Liu, *Nanoscale*, 2021, **13**, 13604–13609.
35 B. Siritanaratkul, M. Forster, F. Greenwell, P. K. Sharma, E. H. Yu and A. J. Cowan, *J. Am. Chem. Soc.*, 2022, **144**, 7551–7556.
36 A. Ozden, F. Li, F. P. García de Arquer, A. Rosas-Hernández, A. Thevenon, Y. Wang, S.-F. Hung, X. Wang, B. Chen, J. Li, J. Wicks, M. Luo, Z. Wang, T. Agapie, J. C. Peters, E. H. Sargent and D. Sinton, *ACS Energy Lett.*, 2020, **5**, 2811–2818.

